

## Supporting Information for

### **Environmental Photochemistry of Altrenogest: Photoisomerization to a Bioactive Product with Increased Environmental Persistence via Reversible Photohydration**

Kristine H. Wammer<sup>†,\*</sup>, Kyler C. Anderson,<sup>†</sup> Paul R. Erickson,<sup>‡</sup> Sarah Kliegman,<sup>‡,\*</sup> Marianna E. Moffatt,<sup>†</sup> Stephanie M. Berg,<sup>†</sup> Jackie A. Heitzman,<sup>§</sup> Nicholas C. Pflug,<sup>¥</sup> Kristopher McNeill,<sup>‡</sup> Dalma Martinovic-Weigelt,<sup>§</sup> Ruben Abagyan,<sup>€</sup> David M. Cwiertny,<sup>‡</sup> Edward P. Kolodziej,<sup>‡,‡</sup>

<sup>†</sup>Department of Chemistry, University of St. Thomas, St. Paul, MN 55105, USA

<sup>‡</sup>Institute of Biogeochemistry and Pollutant Dynamics, ETH Zürich, CH-8092 Zürich, Switzerland

<sup>§</sup>Department of Biology, University of St. Thomas, St. Paul, MN 55105, USA

<sup>¥</sup>Department of Chemistry, University of Iowa, Iowa City, IA 52242, USA

<sup>€</sup>Skaggs School of Pharmacy and Pharmaceutical Sciences, University of California, San Diego, 9500 Gilman, La Jolla, CA 92093-0747.

<sup>‡</sup>Department of Civil and Environmental Engineering, University of Iowa, Iowa City, IA 52242, USA

<sup>‡</sup>Interdisciplinary Arts and Sciences, University of Washington, Tacoma, Tacoma, WA 98402 USA

<sup>‡</sup>Department of Civil and Environmental Engineering, University of Washington, Seattle, WA 98195-2700 USA

\*Corresponding author, Email: khwammer@stthomas.edu, Telephone: 651-962-5574

**Supplemental text: Materials, Altrenogest Photolysis at Environmentally Relevant Concentrations, Quantum Yield Measurements, Laser Flash Photolysis, Altrenogest Photolysis with Humic Acid, Photolysis of Commercial Oil Solutions, Analytical Methods, AR Assay Methods, In Silico Modeling of ALT and ALT Photoproduct Binding with Nuclear Hormone Receptors, Quantum Yield Calculation**

**Figure S1.** Spectral output of the Suntest CPS+ solar simulator with UV filter at an irradiance setting of 750 W/m<sup>2</sup> (data obtained from Atlas Material Testing Technology, LLC).

**Figure S2.** ALT concentration over time for photolysis experiments conducted at an initial ALT concentration of 1.6 nM.

**Figure S3.** ALT concentration over time for photolysis experiments conducted in the presence of 40 and 80 mg/L of Fluka Humic Acid.

**Table S1.** Average observed direct photolysis rate constants ( $k_{\text{obs}}$ ) for 10  $\mu\text{M}$  ALT solutions in solar simulator with irradiance setting of 250  $\text{W}/\text{m}^2$ .

**Figure S4.** First-order kinetic fits used to determine pH-dependence of ALT photolysis rate constant. 10  $\mu\text{M}$  ALT solutions, 30  $^{\circ}\text{C}$ , air-saturated.

**Figure S5.** First-order kinetic fits used to determine temperature-dependence of ALT photolysis rate constant. 10  $\mu\text{M}$  ALT solutions, DI water, air-saturated.

**Figure S6.** First-order kinetic fits used to determine oxygen-dependence of ALT photolysis rate constant. 10  $\mu\text{M}$  ALT solutions, DI water, 30  $^{\circ}\text{C}$ .

**Figure S7.** Example chromatograms illustrating formation of the same product in aqueous solutions and commercial oil solutions of ALT. (a) Unphotolyzed 10  $\mu\text{M}$  aqueous ALT solution. (b) Unphotolyzed 0.22% ALT solution in oil (Regu-Mate<sup>®</sup>) extracted prior to HPLC analysis. (c) 10  $\mu\text{M}$  aqueous ALT solution photolyzed for 20 seconds. The peak at 4.4 minutes is the primary photoproduct (ALT-CAP). (d) Regu-Mate<sup>®</sup> solution photolyzed for 20 minutes, extracted prior to HPLC analysis. The same primary photoproduct (ALT-CAP) is observed. Detection wavelength of 354 nm shown for unphotolyzed solutions; detection wavelength of 320 nm shown for photolyzed solutions.

**Figure S8.** Top panel: Kinetic traces of the decay of triplet state 17 $\beta$ -TBOH and ALT. The black lines indicate the first-order exponential best fit. Bottom panel:  $\Delta$  Abs spectra for  $\Delta$ 17 $\beta$ -TBOH and ALT immediately following excitation.

**Figure S9.** Peak area of primary photoproduct (ALT-CAP, at 320 nm) plotted as percent of initial ALT peak area (at 320 nm) for regeneration at pH 2 (red squares) and pH 12 (blue diamonds). Photolysis was conducted for 10  $\mu\text{M}$  ALT solutions in DI water at 30  $^{\circ}\text{C}$  and then pH-adjusted; time in hours on the x-axis is regeneration time subsequent to this adjustment.

**Table S2.** Concentrations of ALT and ALT-CAP in samples tested in androgenic activity cell assay. Assay was performed on a dilution series of each sample.

**Figure S10.** Dose-response curves for dilution series of solutions of T standard, unphotolyzed ALT, ALT + photoproducts (40 seconds photolysis) and photoproducts only (9 minutes photolysis) solutions for ability to activate AR-mediated gene transcription in MDA-kb2 cells.  $\text{EC}_{50}$  values are reported in mol/L and are calculated using concentration at end of assay.

**Table S3.**  $\text{EC}_{50}$  values for dose-response curve shown in Figure S8 (in mol/L). ALT and ALT + photoproducts (40 s) samples are in terms of ALT concentration; photoproducts (9 min) sample is in terms of ALT-CAP concentration.

**Table S4.** Virtual ligand screening results for ALT and ALT photoproduct binding with the Androgen Receptor (AR) and Progesterone Receptor (PRGR). Values in bold represent binding constants that indicate tight binding and are predicted to be in the nanomolar range given the confidence intervals.

**Table S5.** NMR data for ALT-CAP in deuterated acetonitrile ( $\text{CD}_3\text{CN}$ ) including structure with assignments.

**Table S6.** NMR data for ALT in deuterated acetonitrile ( $\text{CD}_3\text{CN}$ ) including structure with assignments.

**Materials.** ALT (99.9%) was purchased from Sigma-Aldrich. 17 $\beta$ -trenbolone (17 $\beta$ -TBOH) and testosterone (T) were purchased from Steraloids (>99%). Pyridine (99+%) and *p*-nitroanisole (PNA; 99+%) were supplied by Thermo Fisher Scientific. Matrix® was obtained from Valley Vet. Altresyn and Regu-Mate® were acquired through River Basin Equine Veterinary Services. A commercial humic acid (Fluka; Germany) was used in select photolysis experiments. Methylene blue as a chloride salt (>98.5% spectroscopic grade) was purchased from TCI. Buffer components were supplied by VWR or TCI. Assay media components came from Gibco. Lysis buffer was from Ligand Pharmaceuticals. Dispersive SPE tubes were from United Science. Solvents were of HPLC grade. Deionized water was purified using a Barnstead Nanopure system. All gases used were high purity grade (99.999%). All chemicals were used as received.

**Altrenogest Photolysis at Environmentally Relevant Concentration:** 322  $\mu$ L of 10 mM ALT stock solution (in methanol) was added to 1 L of deionized water.

Subsequently, 500  $\mu$ L of this solution was added to another 1 L of deionized water for an initial ALT concentration of ~500 ng/L. Photolysis experiments with the Suntest solar simulator used 600 mL of this 500 ng/L solution, with sacrificial sampling of five identical reactors after 0, 0.1, 0.5, 5, or 15 minutes of irradiation. At the conclusion of each desired irradiation period, the entire content of the reactor (600 mL) was concentrated on a C18 cartridge, and the cartridge was then eluted with 6 mL of acetonitrile. The acetonitrile solution was then evaporated to dryness via a gentle stream of compressed air and the residue was redissolved in 500  $\mu$ L of methanol for analysis by high performance liquid chromatography using an ultraviolet-visible (UV-Vis) diode array detector (HPLC-DAD) (see below for analytical details).

**Altrenogest Photolysis with Humic Acid.** 20  $\mu$ L of 10 mM ALT stock solution (in methanol) was added to a 20 mL solution containing either 40 or 80 mg/L of Fluka Humic Acid (FHA) prepared in 5 mM potassium phosphate buffer (pH 7). This produced an initial ALT concentration of 10  $\mu$ M. This mixture was then photolyzed with a 1000 W Xe Arc lamp equipped with a 305 nm cut-off filter. Samples were periodically collected over time, transferred to an amber autosampler vial, and immediately analyzed by HPLC-DAD.

**Photolysis of Commercial Oil Solutions.** Photolysis of Regu-Mate®, Matrix®, and Altresyn® was performed using the commercial oil solutions as is. For each sample, ALT was extracted prior to analysis. A 20  $\mu$ L aliquot of oil solution was diluted 1:100 in acetonitrile and loaded into a dispersive Solid Phase Extraction tube (dSPE, 2 mL volume, United Science, LLC; Center City, MN) containing 50 mg of C18 functionalized flash silica (30-60 micron). After vortexing and centrifuging, the supernatant was removed and diluted 50:50 with acetonitrile. This solution was then passed through a 0.2  $\mu$ m filter and analyzed by HPLC-DAD.

**Quantum Yield Measurements.** The quantum yield of ALT was determined in deionized water at 30 °C. A UV-Vis absorbance spectrum of ALT solution was obtained using a Thermo Scientific Evolution Array spectrophotometer. A portion of ALT solution was then irradiated in the solar simulator alongside a PNA/pyridine actinometer solution prepared according to Leifer with a quantum yield of 0.0527.<sup>1</sup>

**Laser Flash Photolysis.** Laser flash photolysis (LFP) experiments were carried out in 1 cm cuvettes with solution concentrations of 100  $\mu$ M for both ALT and the TBA metabolite 17 $\beta$ -trenbolone (17 $\beta$ -TBOH). To compensate for its rapid phototransformation, 100 mL of ALT solution was continuously cycled through a flow-through cuvette by a peristaltic pump. Transient decays were extracted and successfully fit to first-order exponentials using Surface Explorer (Ultrafast Systems) or Origin 8.5 (OriginLab). The experimental setup has previously been described in detail.<sup>2</sup> Briefly, experiments were performed using a time-resolved pump-probe transient absorption spectrometer (EOS, Ultrafast Systems). Excitation pulses were generated from the output (795 nm, 1kHz, pulse width <100 fs) of a Ti:sapphire laser (Solstice, Newport Spectra Physics), which was converted to the desired wavelength (350 nm, pulse energy < 5  $\mu$ J) by an optical parametric amplifier (TOPAS-C, Light Conversion).

**Analytical Methods.** ALT concentration and photoproduct peak areas were measured using an Agilent 1100 series HPLC-DAD. An Agilent Eclipse XDB-C18 column (4.6 mm  $\times$  150 mm, 5  $\mu$ m particle size) was used and the mobile phase was 50:50 water:acetonitrile at a 1.0 ml per minute flow rate. ALT was detected at 354 nm, whereas photolysis products were detected at 254 nm and 320 nm.

A Thermo Exactive Orbitrap mass spectrometer with an electrospray ionization source coupled to a Waters nanoACQUITY UPLC was operated in positive ionization mode to characterize some photoproducts. A Waters Atlantis C18 column (3  $\mu$ m) was used with a 50:50 acetonitrile:water mobile phase at 10  $\mu$ L/min. Thermo Xcalibur software was used for data acquisition.

The primary photoproduct of ALT was identified by NMR. A solution of ALT in deuterated acetonitrile (12 mM) was prepared in a sealable NMR tube (Wilmad) and deoxygenated by first freezing, evacuating the tube under high vacuum, then closing the vacuum and thawing the solution (freeze/pump/thaw). This cycle was repeated three times to remove a maximum of dissolved oxygen from the system. The solution in the NMR tube was then photolyzed in a Rayonet photoreactor (Southern New England Ultraviolet Company) containing two 350 nm wavelength bulbs. Reaction progress was tracked using a 400 MHz Bruker Ascend Aeon spectrometer and a BBI 1H/D-BB Z-GRD probe via  $^1\text{H}$  NMR until ALT had been completely transformed into the primary photoproduct (~ 9 min). Conventional  $^1\text{H}$  NMR spectra were measured at 400.13 MHz; chemical shifts are reported in ppm and referenced to residual solvent signal for  $\text{CD}_3\text{CN}$  at  $\delta$   $^1\text{H}$  1.97. Assignments for ALT and the primary photoproduct after complete transformation were carried out using  $^1\text{H}$ ,  $^{13}\text{C}$  DEPT90 and  $^{13}\text{C}$  DEPT135,  $^1\text{H}$ - $^1\text{H}$  COSY,  $^1\text{H}$ - $^{13}\text{C}$  HSQC,  $^1\text{H}$ - $^{13}\text{C}$  HMBC, and  $^1\text{H}$ - $^1\text{H}$  NOESY spectra.

Chemical shifts of carbons in ALT and the photoproduct were measured using distortionless enhancement by polarization transfer (DEPT); spectra were measured at 100.6 MHz and are reported in ppm. The DEPT90 and DEPT135 spectra were acquired using the pulse programs **dept90** and **dept135** with the following parameters: number of scans 3072, spectral width 24038.461 Hz, transmitter frequency offset (observe nucleus  $^{13}\text{C}$ ), 10060.80 Hz, transmitter frequency offset (second nucleus  $^1\text{H}$ , 1600.52 Hz). The C-H coupling constant used was 145 Hz. Quaternary carbon chemical shifts were estimated using correlations from HMBC spectra.

Two-dimensional  $^1\text{H}$ - $^1\text{H}$  COSY (correlation spectroscopy) spectra were acquired using the pulse program **cosygpppqf** with the following parameters: number of scans 32, size of fid 2048 and 128 in f2 and f1, respectively, sweep width 8223.685 Hz, and transmitter offset frequency 2470.97 Hz. Two-dimensional  $^1\text{H}$ - $^1\text{H}$  NOESY were acquired using the pulse program **noesygpphpp** with the following parameters: number of scans 8, number of dummy scans 32, size of fid 2048 and 256 in f2 and f1, respectively, sweep width 8223.685 Hz, and transmitter offset frequency 2470.97 Hz. The relaxation delay was 1 second, and the mixing time was 0.3 seconds. The gradient shape was SMSQ10.100, the gradient strength for GPZ1 was 40%, and the gradient pulse length p16 was 1000  $\mu\text{s}$ .

Two-dimensional inverse-detected  $^1\text{H}$ - $^{13}\text{C}$  heteronuclear correlation (HSQC, heteronuclear single quantum correlation) NMR spectra were acquired using the pulse program **hsqcetgp** with the following parameters: number of scans 16, number of dummy scans 16, size of fid 1024 and 256 in  $^1\text{H}$  and  $^{13}\text{C}$  dimensions, respectively, sweep width 8223.685 Hz and 16666.666 Hz in  $^1\text{H}$  and  $^{13}\text{C}$  dimensions, respectively, and transmitter offset frequency 2470.97 Hz and 7503.73 Hz in  $^1\text{H}$  and  $^{13}\text{C}$  dimensions, respectively. The gradient shape was SINE.100, and the gradient strengths for GPZ1 and GPZ2 were 80% and 20.1%, respectively, and the gradient pulse length p16, was 100  $\mu\text{s}$ . The HMBC (heteronuclear multiple bond correlation) NMR spectra were acquired using the pulse program **hmbcgplpndqf** with the following parameters: number of scans 16, number of dummy scans 16, size of fid 2048 and 128 in  $^1\text{H}$  and  $^{13}\text{C}$  dimensions, respectively, sweep width 8223.685 Hz and 22347.830 Hz in  $^1\text{H}$  and  $^{13}\text{C}$  dimensions, respectively, and transmitter offset frequency 2470.97 Hz and 1004431 Hz in  $^1\text{H}$  and  $^{13}\text{C}$  dimensions,



respectively. The gradient shape was SMSQ10.100, and the gradient strengths for GPZ1, GPZ2, GPZ3 were 70%, 30%, and 65.15%, respectively, and the gradient pulse length p16, was 1000  $\mu$ s.

**AR Assay Methods.** Cells were maintained in L-15 media enriched with 10% Fetal Bovine Serum and 1% Antibiotic/Antimycotic solution at 37 °C without carbon dioxide. For the assay, cells were added to 96-well luminometer plates at a concentration of 50,000 cells per well and incubated in the dark at 37 °C for 4 hours prior to addition of test solutions.

The dilution series of T standard solutions ( $10^{-8}$  to  $10^{-12}$  M) was prepared in 100% methanol and then diluted further into supplemented L-15 media prior to addition to the wells. Similarly, a series of solutions ( $10^{-6}$  to  $10^{-16}$ ) was prepared from  $10^{-5}$  M aqueous ALT (0.1% methanol cosolvent) diluted in water and then media, and added to the wells. Cells were incubated with the test solutions at 37 °C for 18 hours and then lysed with lysis buffer. Luminescence (relative light units) was measured with a luminometer (Synergy 2, BioTek) after the addition of reaction buffer and luciferin. A Live/Dead viability/cytotoxicity kit (Invitrogen) was used per manufacturer instructions to screen for cytotoxicity. ALT concentrations prior to and after incubation were measured by HPLC using a standard curve. Because UV-Vis absorbance data showed similar molar absorptivity for ALT-CAP and ALT at their respective  $\lambda_{\text{max}}$  values, ALT-CAP concentrations were estimated based on HPLC peak area at 320 nm using the same standard curve. ALT concentrations and ALT-CAP concentration estimates are listed in Table S3.

In addition, a series of assays was performed with 2-hydroxyflutamide (an androgen receptor antagonist) spiked to T and ALT solutions to verify that observed transcriptional activity in the absence of 2-hydroxyflutamide was due to AR rather than glucocorticoid receptor (GR) binding, as MDA-kb2 cells also express GR. The relative androgenic activity of photoproducts/mixtures was calculated by: 1) expressing it as a percent of maximum response to T standards, or as 2) effective concentration needed to exert 50% of the maximum response for a photoproduct/mixture of interest ( $EC_{50}$ ). To identify maximum T response and  $EC_{50}$  values for T, ALT and photoproducts/mixtures, a nonlinear sigmoidal dose-response curve was fit to the relative luminescence units of the T, ALT and photoproducts/mixtures run at multiple dilutions (using Prism 5.02., Graph Pad Software Inc.).

**In Silico Modeling of ALT and ALT Photoproduct Binding with Nuclear Hormone Receptors.** Virtual target screening by ligand docking is an *in silico* computational method that uses a panel of three-dimensional molecular docking models to screen target structures (i.e. transformation products). The full panel, that included estrogen and progesterone receptors, is based on the “pocketome”, a computational library of over 2600 protein binding sites that represent drug/toxicant targets.<sup>3-6</sup> This predicts binding poses of ligands under study as three-dimensional molecular structures, then employs computational models trained on known ligands with their binding constants.<sup>5</sup> The prediction reliability is estimated by two different methods: (a) via the probability (p-value) of the observed score deviation from the mean calculated from scores of 6000 known drugs, the confidence intervals for  $K_d$  values derived from cross-validation of the

models. Receptor binding affinity constants ( $pK_d$ ) also are estimated together with the confidence intervals. Virtual docking was conducted for ALT and photoproducts (ALT-CAP and ALT-CAP-OH) against both androgen and progesterone receptors. For ALT-CAP-OH, hydration was presumed to occur at the C5 position in the steroid A-ring.

**Quantum Yield Calculation.** An absorbance spectrum for ALT was used in conjunction with emission intensities for the lamp/filter in the solar simulator to calculate the quantum yield for this ALT solution for the wavelength range 296-450 nm using Equation 1

$$\Phi_{alt} = \Phi_{act} \left[ \frac{k_{alt} \sum L_{\lambda} \varepsilon_{\lambda, act}}{k_{act} \sum L_{\lambda} \varepsilon_{\lambda, alt}} \right] \quad (1)$$

where  $\Phi$  denotes quantum yield,  $k$  is  $k_{obs}$ ,  $L_{\lambda}$  is the light intensity at a specific wavelength, and  $\varepsilon_{\lambda}$  is the molar absorptivity at that wavelength for a *p*-nitroanisole/pyridine (PNA) actinometer solution (subscript act) photolyzed alongside ALT (subscript alt).

## REFERENCES

- (1) Leifer, A. *The Kinetics of Environmental Aquatic Photochemistry, Theory and Practice*; American Chemical Society: Washington, D.C., USA, 1988.
- (2) Wenk, J.; Eustis, S.N.; McNeill, K.; Canonica, S. Quenching of excited triplet states by dissolved natural organic matter. *Environ. Sci. Technol.* **2013**, *47*, 12802-12810.
- (3) Kufareva, I.; Ilatovskiy, A.V.; Abagyan, R. Pocketome: an encyclopedia of small-molecule binding sites in 4D. *Nucleic Acids Res.* **2012**, *40*, D535-D540.
- (4) Chen, Y.C.; Totrov, M.; Abagyan, R. Docking to multiple pockets or ligand fields for screening, activity prediction and scaffold hopping. *Future Med. Chem.* **2014**, *6*, 1741-1755.
- (5) McRobb, R.M.; Kufareva, I.; Abagyan, R. In silico identification and pharmacological evaluation of novel endocrine disrupting chemicals that act via the

ligand-binding domain of the estrogen receptor alpha. *Toxicol. Sci.* **2014**, *141*, 188-197.

(6) Park, S.J.; Kufareva, I.; Abagyan, R. Improved docking, screening and selectivity prediction for small molecule nuclear receptor modulators using conformational ensembles. *J. Comput. Aided Mol. Des.* **2010**, *71*, 459-71.

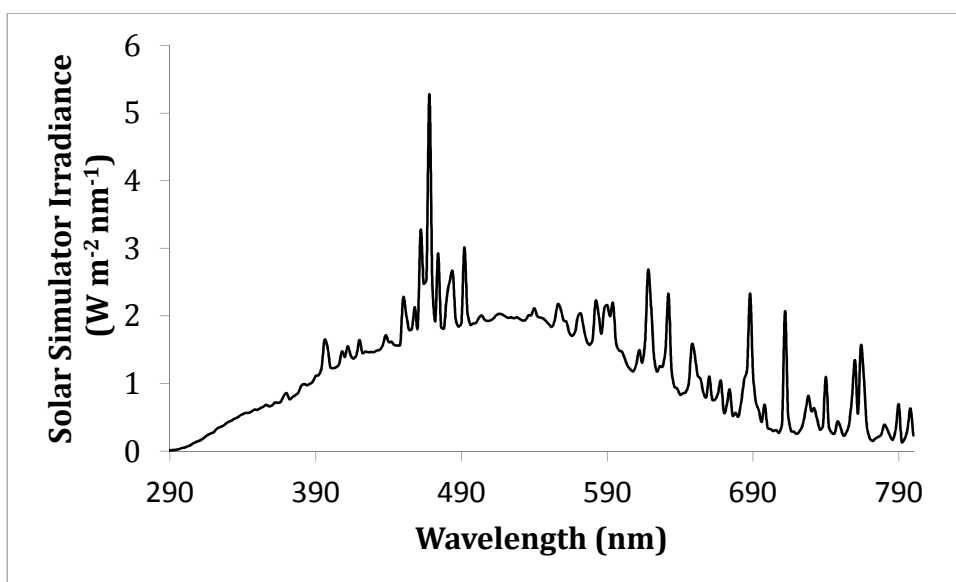


**Figure S1.** Spectral output of the Suntest CPS+ solar simulator with UV filter at an irradiance setting of 750 W/m<sup>2</sup> (data obtained from Atlas Material Testing Technology, LLC).

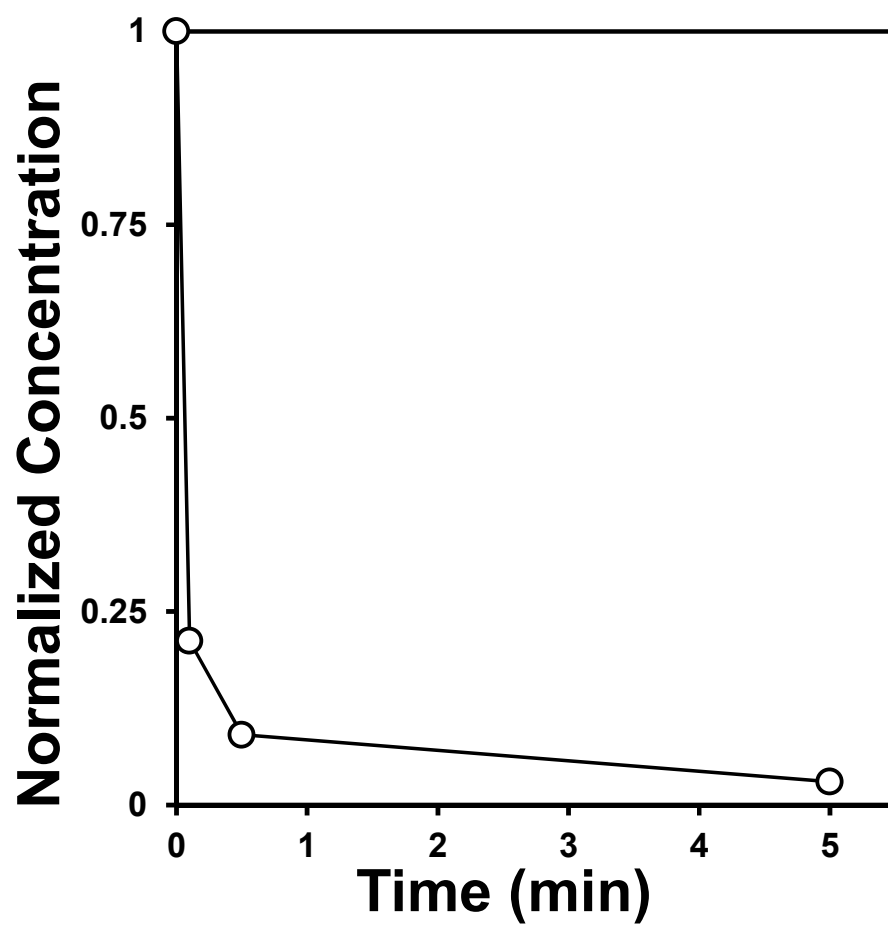


**Figure S2.** ALT concentration over time for photolysis experiments conducted at an initial ALT concentration of 1.6 nM.

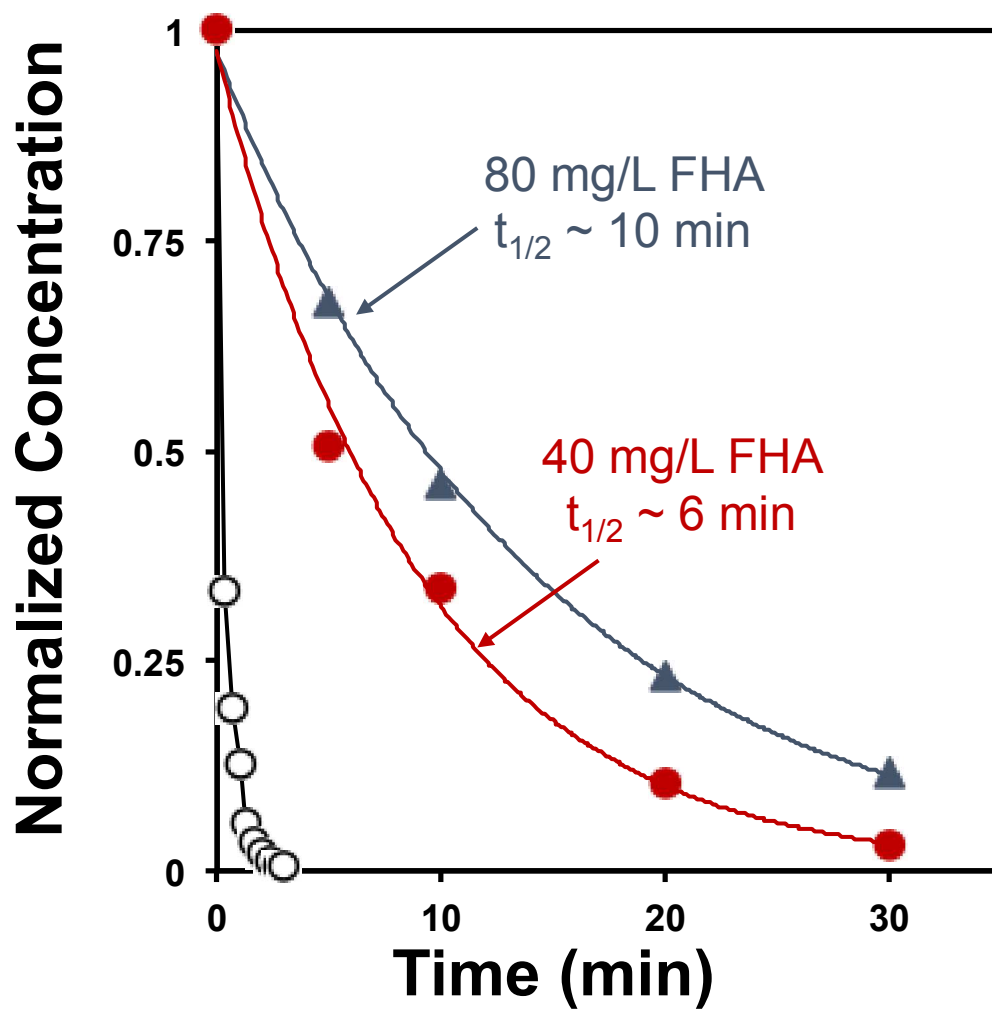


**Figure S3.** ALT concentration over time for photolysis experiments conducted in the presence of 40 mg/L (red circles) and 80 mg/L (grey triangles) of Fluka Humic Acid. Data for an air-saturated system with no humic acid present from Figure 1 (open circles) are included for comparison.

**Table S1.** Average observed direct photolysis rate constants ( $k_{\text{obs}}$ ) for 10  $\mu\text{M}$  ALT solutions in solar simulator with irradiance setting of 250  $\text{W}/\text{m}^2$ .

<b>30 °C, air-saturated</b>	
pH <sup>a</sup>	$k_{\text{obs}} (\text{s}^{-1})/10^{-2}$
3.7 $\pm$ 0.2	2.47 $\pm$ 0.02
5.7 $\pm$ 0.2	2.77 $\pm$ 0.14
9.3 $\pm$ 0.2	2.53 $\pm$ 0.13
<b>Unadjusted pH, air-saturated</b>	
Temperature <sup>b</sup>	$k_{\text{obs}} (\text{s}^{-1})/10^{-2}$
30 °C	2.58 $\pm$ 0.04
32 °C	3.00 $\pm$ 0.08
35 °C	2.61 $\pm$ 0.04
40 °C	2.95 $\pm$ 0.04
44 °C	2.51 $\pm$ 0.05
<b>30 °C, unadjusted pH</b>	
Oxygen level <sup>a</sup>	$k_{\text{obs}} (\text{s}^{-1})/10^{-2}$
N <sub>2</sub> -saturated	9.10 $\pm$ 0.32
O <sub>2</sub> -saturated	1.38 $\pm$ 0.11

<sup>a</sup>Average and standard deviation of three trials

<sup>b</sup>Average and standard deviation of two trials

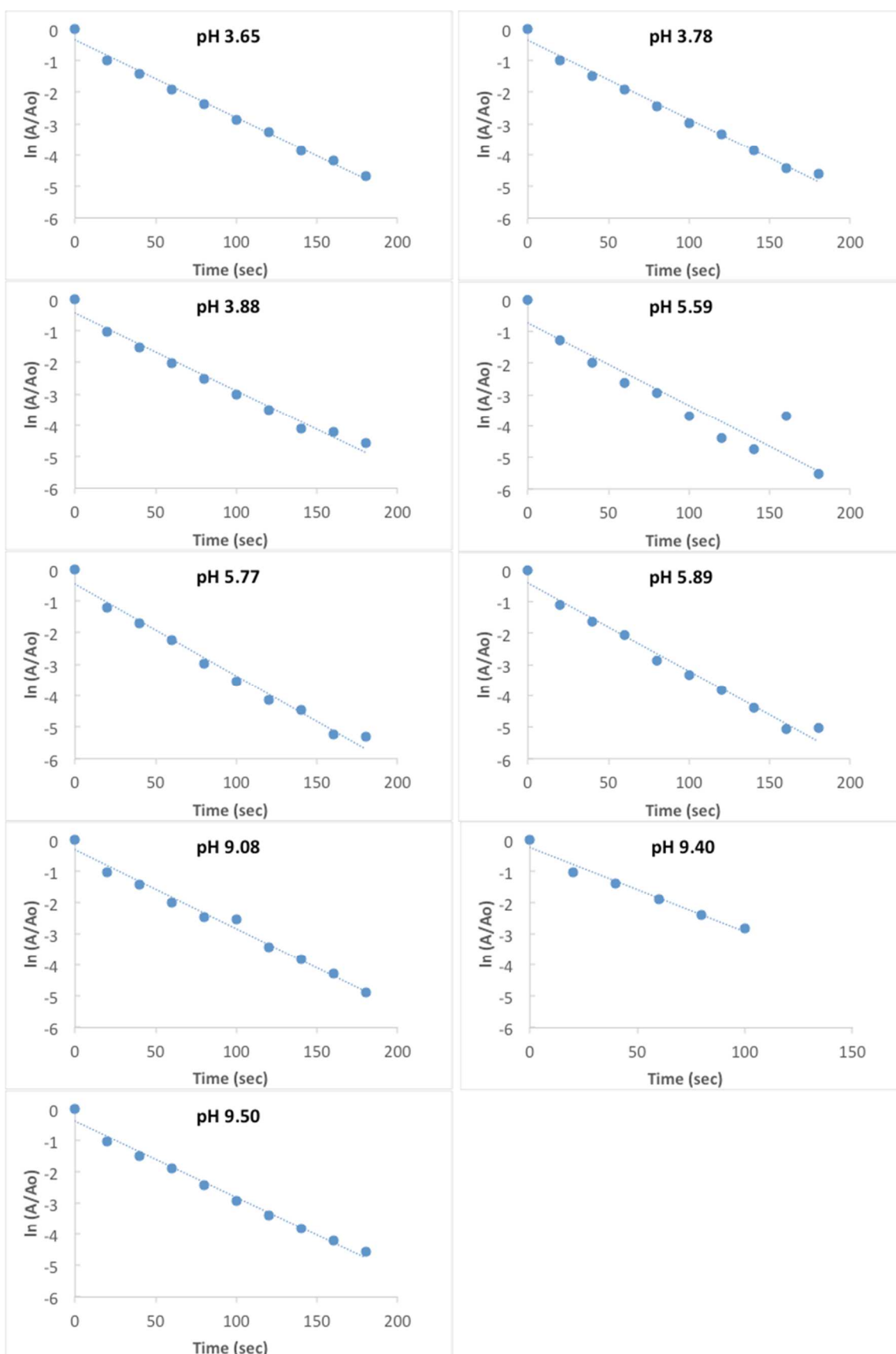


**Figure S4.** First-order kinetic fits used to determine pH-dependence of ALT photolysis rate constant. 10  $\mu$ M ALT solutions, 30  $^{\circ}$ C, air-saturated.



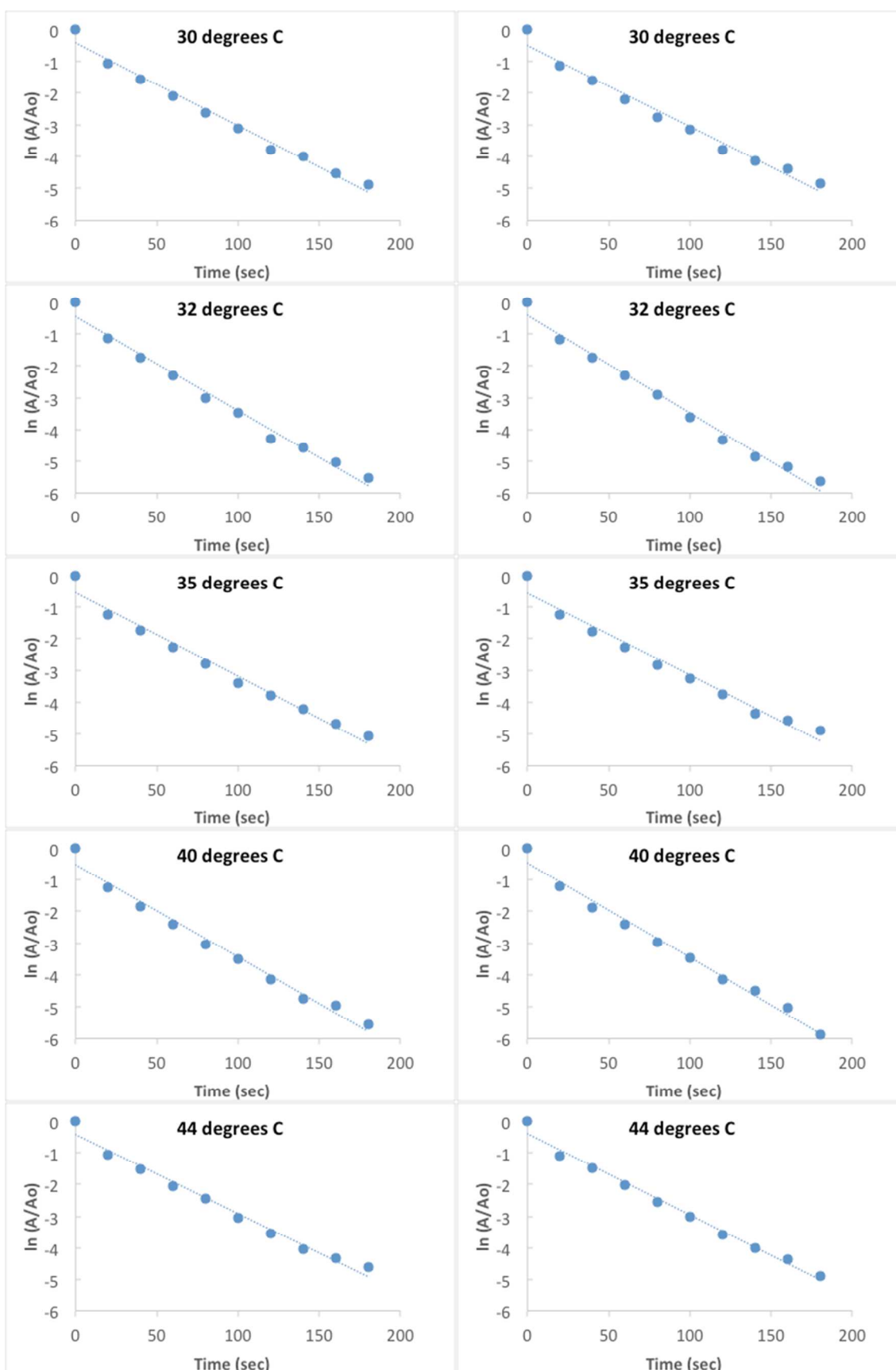


**Figure S5.** First-order kinetic fits used to determine temperature-dependence of ALT photolysis rate constant. 10  $\mu$ M ALT solutions, DI water, air-saturated.

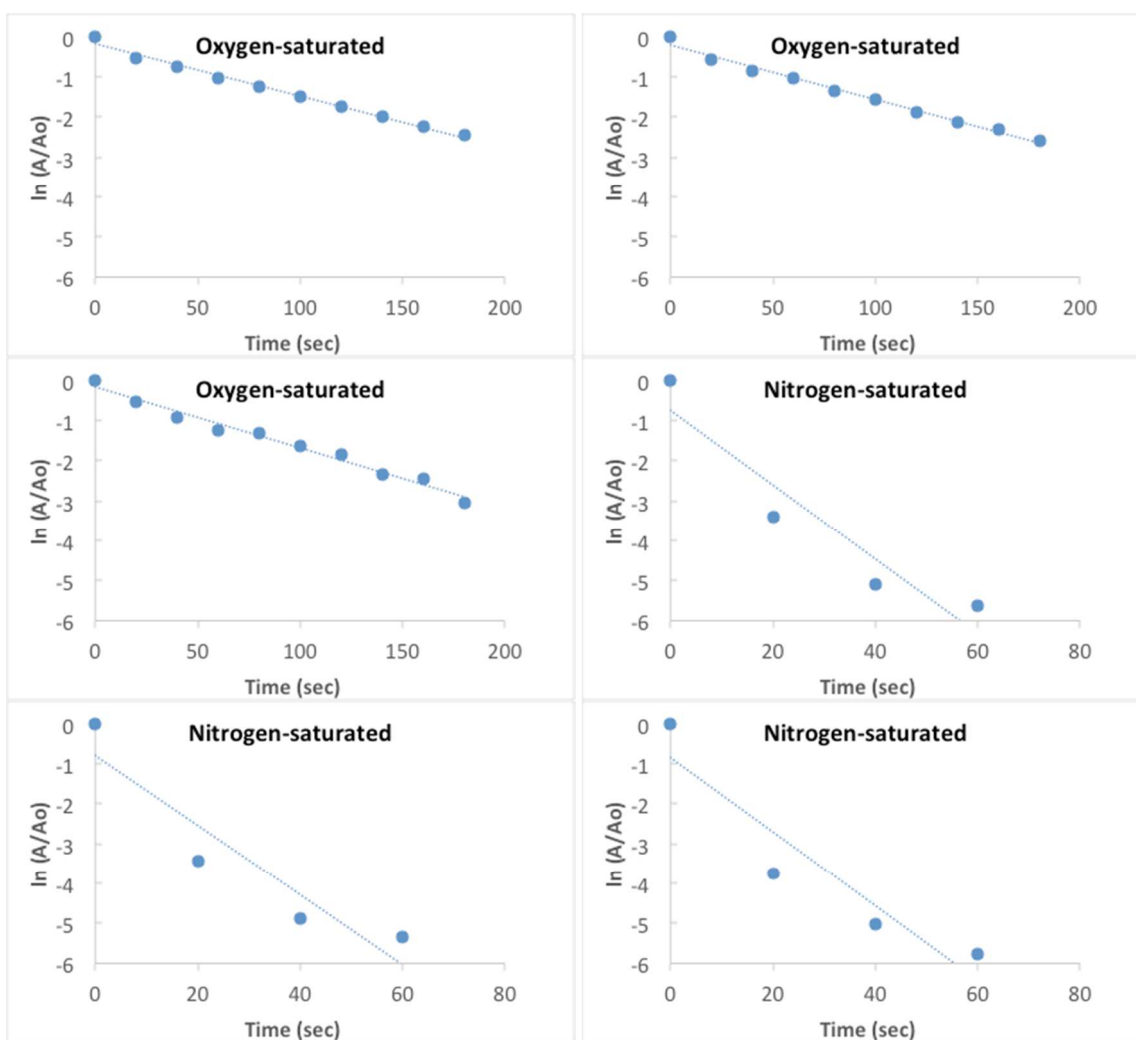


**Figure S6.** First-order kinetic fits used to determine oxygen-dependence of ALT photolysis rate constant. 10  $\mu$ M ALT solutions, DI water, 30  $^{\circ}$ C.

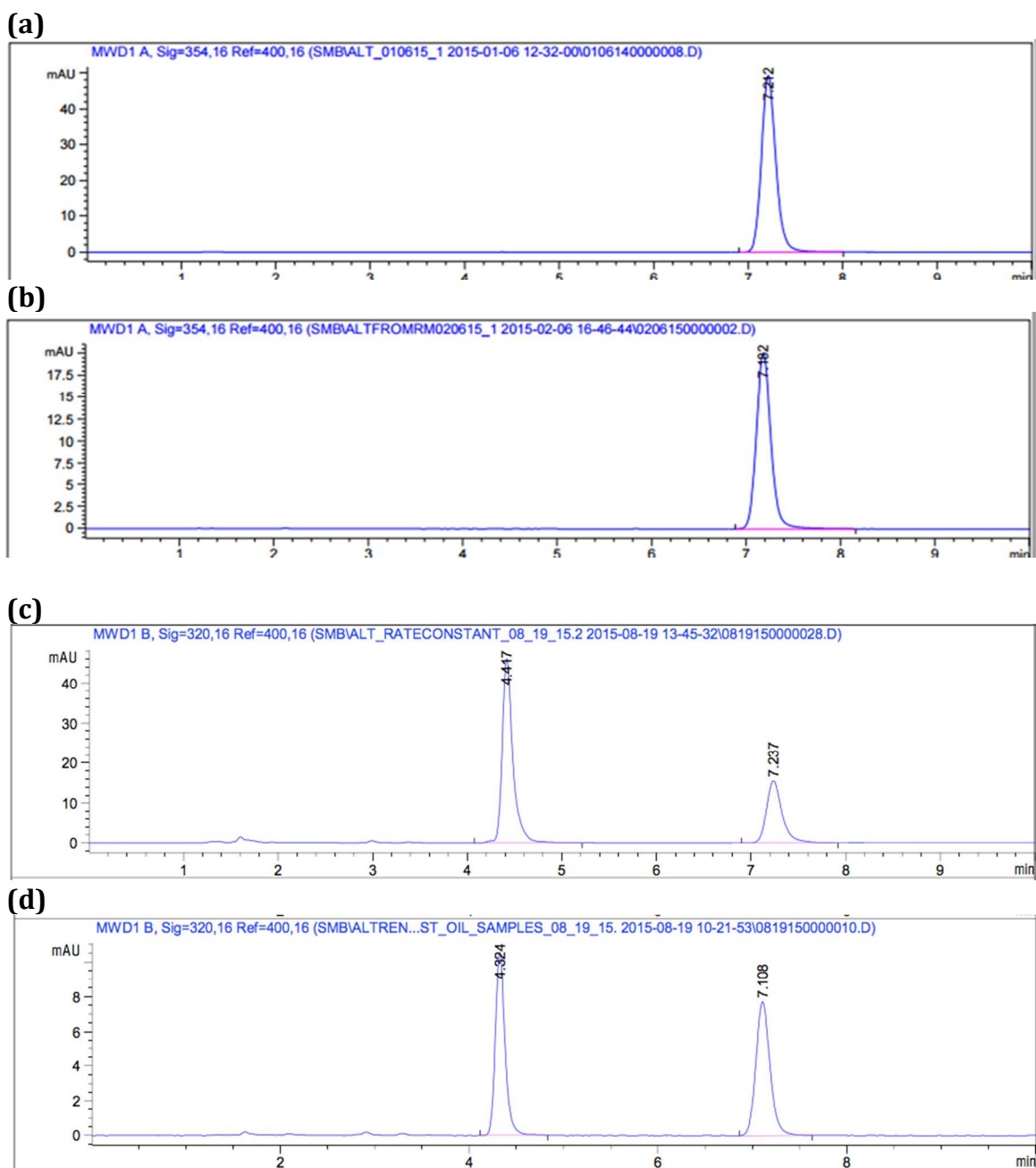


**Figure S7.** Example chromatograms illustrating formation of the same product in aqueous solutions and commercial oil solutions of ALT. (a) Unphotolyzed 10  $\mu$ M aqueous ALT solution. (b) Unphotolyzed 0.22% ALT solution in oil (Regu-Mate®) extracted prior to HPLC analysis. (c) 10  $\mu$ M aqueous ALT solution photolyzed for 20 seconds. The peak at 4.4 minutes is the primary photoproduct (ALT-CAP). (d) Regu-Mate® solution photolyzed for 20 minutes, extracted prior to HPLC analysis. The same primary photoproduct (ALT-CAP) is observed. Detection wavelength of 354 nm shown for unphotolyzed solutions; detection wavelength of 320 nm shown for photolyzed solutions.

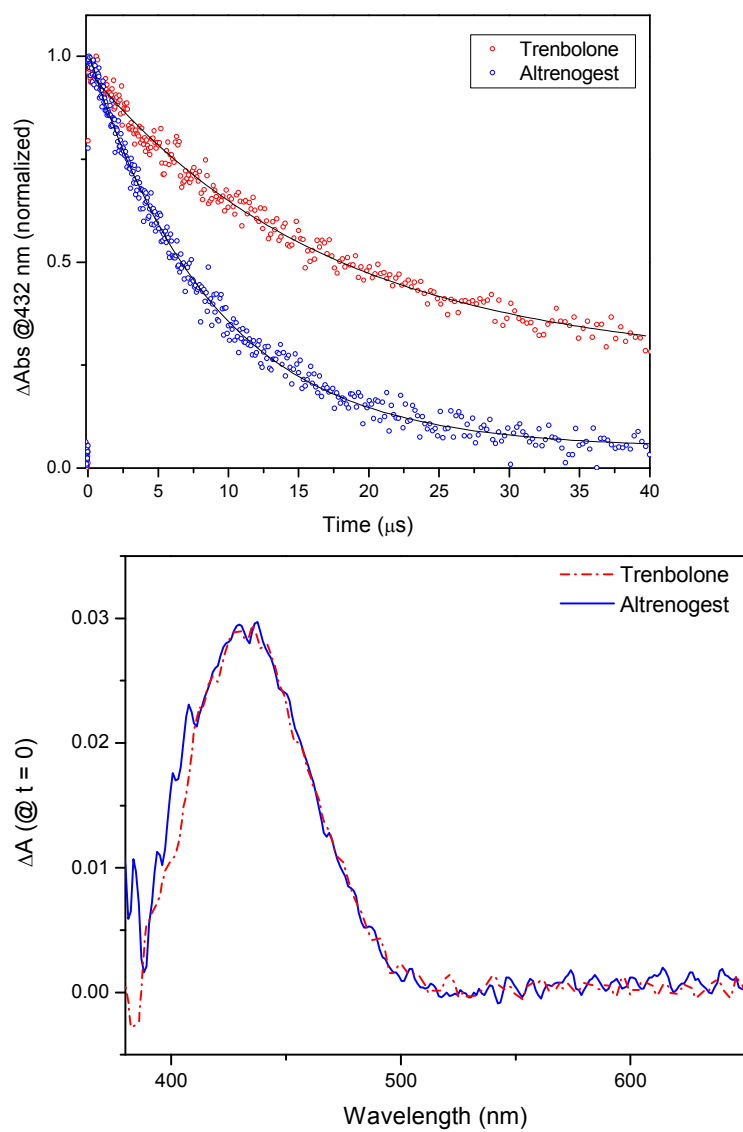


**Figure S8.** Top panel: Kinetic traces of the decay of triplet state  $17\beta$ -TBOH and ALT. The black lines indicate the first-order exponential best fit. Bottom panel:  $\Delta$  Abs spectra for  $\Delta 17\beta$ -TBOH and ALT immediately following excitation.

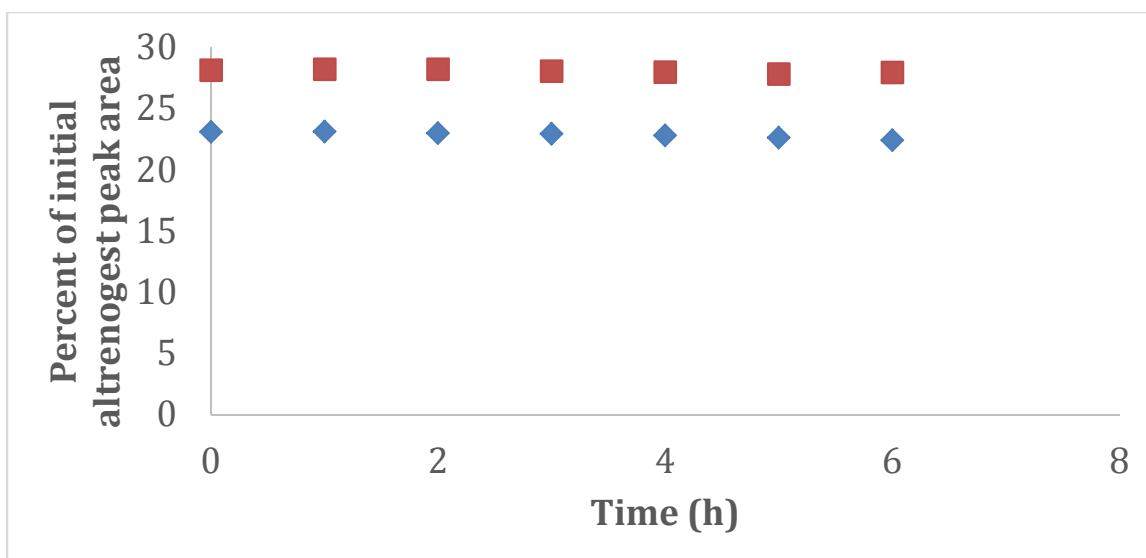


**Figure S9.** Peak area of primary photoproduct (ALT-CAP, at 320 nm) plotted as percent of initial ALT peak area (at 320 nm) for regeneration at pH 2 (red squares) and pH 12 (blue diamonds). Photolysis was conducted for 10  $\mu$ M ALT solutions in DI water at 30  $^{\circ}$ C and then pH-adjusted; time in hours on the x-axis is regeneration time subsequent to this adjustment.

**Table S2.** Concentrations of ALT and ALT-CAP in samples tested in androgenic activity cell assay. Assay was performed on a dilution series of each sample.

Sample	[ALT] (M) <sup>a</sup>	[ALT-CAP] (M) at beginning of assay	[ALT-CAP] (M) at end of assay
Unphotolyzed ALT	$1.0 \times 10^{-6}$	-	-
40 s photoproducts	$1.2 \times 10^{-7}$	$1.8 \times 10^{-7}$	$2.3 \times 10^{-7}$
9 min photoproducts	-	$2.8 \times 10^{-8}$	$2.2 \times 10^{-7}$
Regeneration	-	$1.7 \times 10^{-7}$	$1.7 \times 10^{-7}$

<sup>a</sup>ALT concentrations did not change measurably over the time period of the assay.

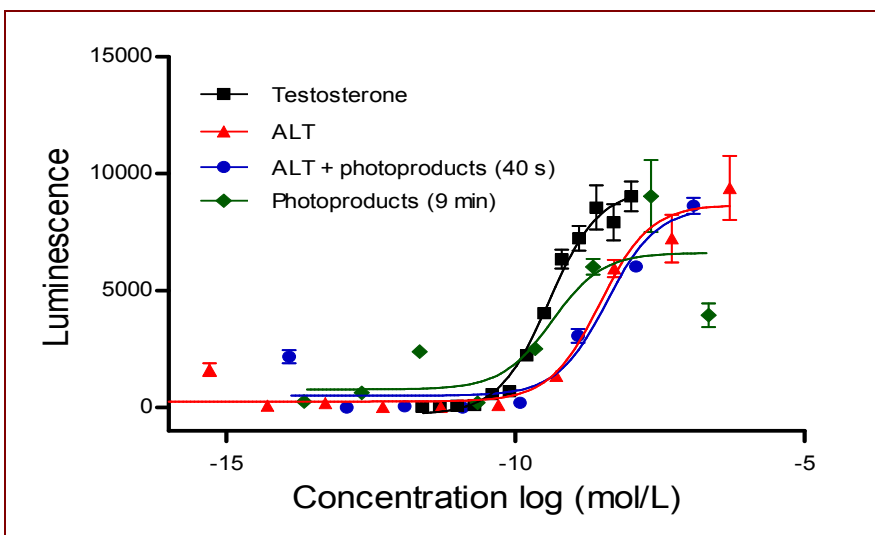


**Figure S10.** Dose-response curves for dilution series of solutions of T standard, unphotolyzed ALT, ALT + photoproducts (40 seconds photolysis) and photoproducts only (9 minutes photolysis) solutions for ability to activate AR-mediated gene transcription in MDA-kb2 cells. EC<sub>50</sub> values are reported in mol/L and are calculated using concentration at end of assay.

**Table S3.** EC<sub>50</sub> values for dose-response curve shown in Figure S8 (in mol/L). ALT and ALT + photoproducts (40 s) samples are in terms of ALT concentration; photoproducts (9 min) sample is in terms of ALT-CAP concentration.

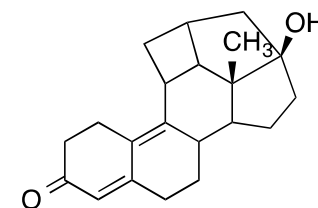
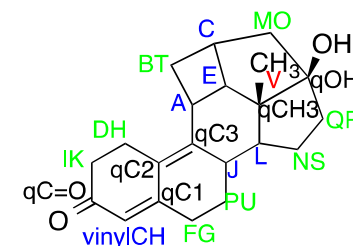
Chemical/mixture	EC50 (mol/L)
Testosterone	3.74E-10
ALT	2.89E-09
ALT + photoproducts (40 s)	3.80E-09
Photoproducts (9 min)	4.27E-10

**Table S4.** Virtual ligand screening results for ALT and ALT photoproduct binding with the Androgen Receptor (AR) and Progesterone Receptor (PRGR). Values in bold represent binding constants that indicate tight binding and are predicted to be in the nanomolar range given the confidence intervals.

<b>Compound</b>	<b>Androgen Receptor</b>		<b>Progesterone Receptor</b>	
	<b>-log(p-value)</b>	<b>p<i>K</i><sub>d</sub> values</b>	<b>-log(p-value)</b>	<b>p<i>K</i><sub>d</sub> values</b>
ALT	3.44	<b>8.5</b>	4.48	<b>9.4</b>
ALT-CAP	4.54	<b>9.4</b>	2.72	<b>7.8</b>
ALT-CAP-OH	1.30	5.2	1.49	5.3

**Table S5.** NMR data for ALT-CAP in deuterated acetonitrile (CD<sub>3</sub>CN) including structure with assignments.

Entry	$\delta^1_{\text{H}}$ <sup>a</sup>	$\delta^{13}_{\text{C}}$ <sup>b</sup>	DEPT 135	HSQC	HMBC 2-bond (H→C)	HMBC 3-bond (H→C)	NOESY
A	3.526	32.17	CH		BT, E, qC3	qCH3, J, qC2	B, E, D
B	3.01	41.91	CH <sub>2</sub>	T		E, qC3	A
C	2.801	34.51	CH				O
D	2.708	25.84	CH <sub>2</sub>	H	IK, qC2	qC=O, qC3, qC1	A
E	2.673	49.46	CH		C, qCH3, A	BT, MO, L, V, qC3	A
F	2.543	32.36	CH <sub>2</sub>	G	U, qC1	J	PU
G	2.497	32.36	CH <sub>2</sub>	F	U, qC1	J, qC2	
H	2.434	25.84	CH <sub>2</sub>	D	IK, qC2	qC=O, qC3, qC1	
I	2.35	37.81	CH <sub>2</sub>	K	DH, qC=O	qC2	
J	2.327	38.92	CH		qC3, L	qC2, qCH3, IK	V
K	2.28	37.81	CH <sub>2</sub>	I	DH, qC=O	qC2	
L	2.213	47.01	CH		qCH3, IK, J	qOH, V, QR, qC3	N, S
M	2.153	53.53	CH <sub>2</sub>	O	C, qOH	BT, qCH3, QR	
N	2.134	37.39	CH <sub>2</sub>	S	L, QR	qCH3, qOH	S
O	2.072	53.53	CH <sub>2</sub>	M	C, qOH	BT, qCH3, QR	C
P	1.874	29.6	CH <sub>2</sub>	U		qC3	F, U
Q	1.751	25.31	CH <sub>2</sub>	R	NS, qOH	L, MO, qCH3	
R	1.681	25.31	CH <sub>2</sub>	Q	NS, qOH	L, MO, qCH3	V
S	1.672	37.39	CH <sub>2</sub>	N	L, QR	qCH3, qOH	L, N
T	1.548	41.91	CH <sub>2</sub>	B	A, C	MO	B
U	1.25	29.6	CH <sub>2</sub>	P	FG, J		F, P
V	0.916	13.28	CH <sub>3</sub>		qCH3	E, qOH, L	J
vinylCH	5.597	122.66	CH			FG, IK, qC2	F
qC=O		198.03			IK	DH	
qC1		156.56			FG	DH	
qC2		117.16			DH, A	J, IK, vinylCH	
qC3		152.99			A, BT	DH, L, PU	
qCH3		57.93			L	MO, NS, QR, A	
qOH		90.39			MO, QR	L, V	

<sup>a</sup>400.13 MHz, <sup>b</sup>100.6 MHz



**Table S6.** NMR data for ALT in deuterated acetonitrile (CD<sub>3</sub>CN) including structure with assignments.

Entry	$\delta^1_{\text{H}}$ <sup>a</sup>	$\delta^{13}_{\text{C}}$ <sup>b</sup>	DEPT 135	HSQC	COSY
A	6.553 (d, <i>J</i> = 9.96 Hz)	125.01	CH		B
B	6.404 (d, <i>J</i> = 10.0 Hz)	143.27	CH		A
C	5.975 (m)	136.61	CH		E, F, N, O
D	5.711 (s)	124.33	CH		-
E	5.14 (d, <i>J</i> = 7.68 Hz)	118.72	CH <sub>2</sub>	F	C, F
F	5.101 (d, <i>J</i> = 15.6 Hz)	118.72	CH <sub>2</sub>	E	C, E
G	2.871 (m)	25.48	CH <sub>2</sub>	H	H, L, M
H	2.81 (m)	25.38	CH <sub>2</sub>	G	G, L, M
I	2.612 (m)	32.43	CH <sub>2</sub>	J	J, Q, V
J	2.574 (m)	32.43	CH <sub>2</sub>	I	I, Q, V
K	2.506 (m)	39.55	CH		R
L	2.392 (m)	37.78	CH <sub>2</sub>	M	G, H, L
M	2.392 (m)	37.78	CH <sub>2</sub>	L	G, H, M
N	2.316 (m)	48.83	CH <sub>2</sub>	O	O
O	2.119 (m)	48.83	CH <sub>2</sub>	N	N
P	2.005 (m)	35.22	CH <sub>2</sub>	T	T
Q	1.931 (m)	28.41	CH <sub>2</sub>	V	I, J, V
R	1.738 (m)	49.27	CH		K
S	1.644 (m)	24.11	CH <sub>2</sub>	U	U
T	1.586 (m)	35.22	CH <sub>2</sub>	P	P
U	1.5 (m)	24.11	CH <sub>2</sub>	S	S
V	1.279 (m)	28.41	CH <sub>2</sub>	Q	I, J, Q
W	0.988 (s)	17.62	CH <sub>3</sub>		-
qC=O		198.12*			
qC1		156.54*			
qC2		135.23*			
qC3		141.89*			
qCH3		48.52*			
qOH		81.17*			

<sup>a</sup>400.13 MHz, <sup>b</sup>100.6 MHz, \*Assigned using <sup>13</sup>C spectrum by analogy to photoproduct since HMBC was unsuccessful.